Stem Cell Reports, Volume *10*

Supplemental Information

Real-Time Monitoring of Glutathione in Living Cells Reveals that High Glutathione Levels Are Required to Maintain Stem Cell Function

Eui Man Jeong, Ji-Hye Yoon, Jisun Lim, Ji-Woong Shin, A. Young Cho, Jinbeom Heo, Ki Baek Lee, Jin-Haeng Lee, Won Jong Lee, Hyo-Jun Kim, Young Hoon Son, Seok-Jin Lee, Sung-Yup Cho, Dong-Myung Shin, Kihang Choi, and In-Gyu Kim

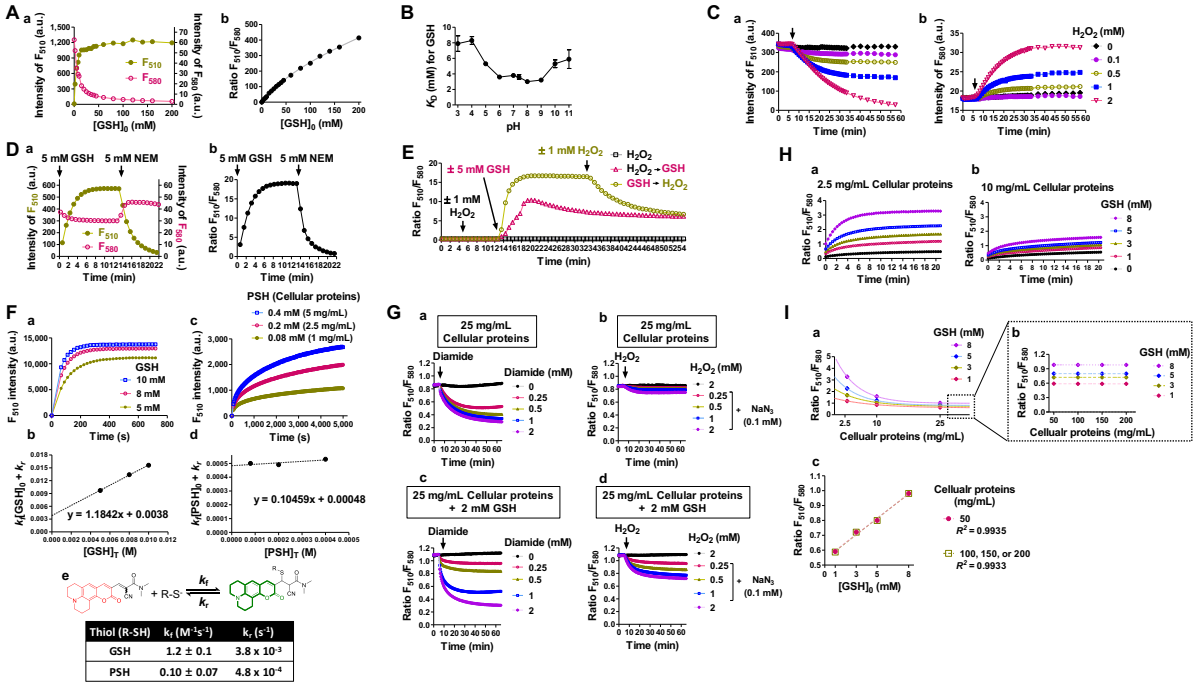

Thiol (R-SH)	k_f ($M^{-1}s^{-1}$)	k_r (s^{-1})
GSH	1.2 ± 0.1	3.8×10^{-3}
PSH	0.10 ± 0.07	4.8×10^{-4}

Figure S1. Properties of FreSHtracer as a Reversible and Ratiometric Glutathione (GSH) Sensor, Related to Figure 1

(A) Relationship between the fluorescence intensity of FreSHtracer and the GSH concentration. (a) Fluorescence emission intensities of FreSHtracer, at 510 nm (F_{510}) and 580 nm (F_{580}), plotted against the GSH concentration. (b) F_{510}/F_{580} ratio (FR) plotted against the GSH concentration. The corresponding fluorescence spectra are shown in Figure 1A.

(B) Effects of pH on the K_D of FreSHtracer for GSH. The K_D values were calculated using SigmaPlot 2000 (SPSS; See **Supplemental Experimental Procedures**).

(C) FreSHtracer (10 μM) was reacted with 5 mM GSH for 20 min. Following treatment with the indicated concentrations of H_2O_2 at room temperature, (a) F_{510} and (b) F_{580} were monitored. The corresponding FR values are shown in Figure 1D.

(D) Rapid and reversible changes of FreSHtracer fluorescence following treatment with GSH or *N*-ethylmaleimide (NEM). (a,b) FreSHtracer was reacted at room temperature (RT), first with 5 mM GSH, and then with 5 mM NEM. The reaction was monitored by recording the F_{510} and F_{580} values (a) and by calculating the FR (b).

(E) FreSHtracer was incubated sequentially with 1 mM H_2O_2 and 5 mM GSH, as indicated. The FR was monitored for 1 h.

(F) Rate constants for the reactions between FreSHtracer and thiols (See **Supplemental Experimental Procedures**). FreSHtracer was added to (a, b) GSH, or (c, d) dialyzed cell lysates (PSH), and F_{510} was monitored.

(e) The calculated rate constants

(G) Monitoring the FR of FreSHtracer in dialyzed cell lysates following treatment with diamide or H_2O_2. (a, b) In dialyzed cell lysates (25 mg/mL protein) equilibrated with FreSHtracer (10 μM, 2 h), the FR was monitored for 1 h following treatment with the indicated amounts of diamide or H_2O_2. (c, d) Dialyzed cell lysates (25 mg/mL protein) spiked with 2 mM GSH were equilibrated with FreSHtracer (10 μM; 2 h) and then the FR was monitored for 1 h following treatment with the indicated amounts of diamide or H_2O_2. Sodium azide was used to inhibit catalase activity in the dialyzed cell lysates (b, d). See also Figure 1H and 1K.

(H) Effect of PSH concentrations on FR_{GSH}. Dialyzed cell lysates (a, 2.5 mg/mL; b, 10 mg/mL) were spiked with various concentrations of GSH and were equilibrated with 10 μM FreSHtracer. The FR was monitored for 20 min. All reactions were performed at room temperature in 10 mM phosphate buffer (pH 7.4) containing 150 mM NaCl and 2% DMSO. a.u., arbitrary units. See also Figure 1I for 25 mg/mL cellular proteins and Figure 1J for the relationship between FR and GSH concentration in PSH-GSH mixtures.

(I) The F_{510}/F_{580} ratio becomes less sensitive at higher protein concentration ranges. All graphs are redrawn from Figure 1J. (a) The F_{510}/F_{580} ratios are curve-fitted and (b) extrapolated to the one phase decay model (GraphPad Prism 5.0): $Y = (Y_0 - \text{plateau}) * \exp(-K * X) + \text{plateau}$. (c) The calculated plateau ratios are plotted against the GSH concentrations. The ratio is expected to be linearly dependent on the GSH level, but not significantly affected by protein concentration changes (50—200 mg/mL).

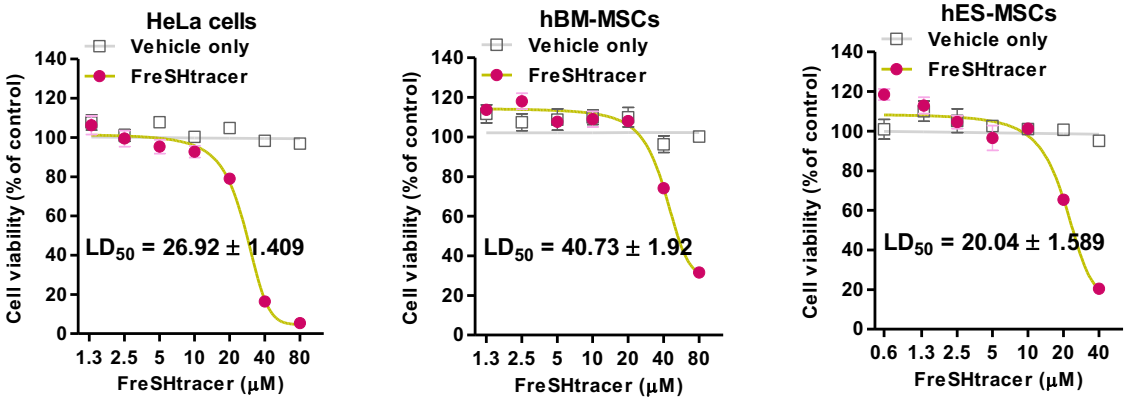

Figure S2. Effects of FreSHtracer on Cell Viability, Related to Figure 2

HeLa cells (5×10^3 cells/well; n = 3 independent biological replicates), hBM-MSCs (1.3×10^3 cells/well; n = 3 independent biological replicates), and hES-MSCs (1×10^4 cells/well; n = 3 independent biological replicates) were cultured for 18 h in 96-well dishes, and then treated for 24 h with either vehicle (dimethyl sulfoxide [DMSO]) or the indicated concentrations of FreSHtracer. Cell viability was analyzed using the MTT method. The LD_{50} values for FreSHtracer were calculated using GraphPad Prism 5. All error bars represent the mean ± SEM.

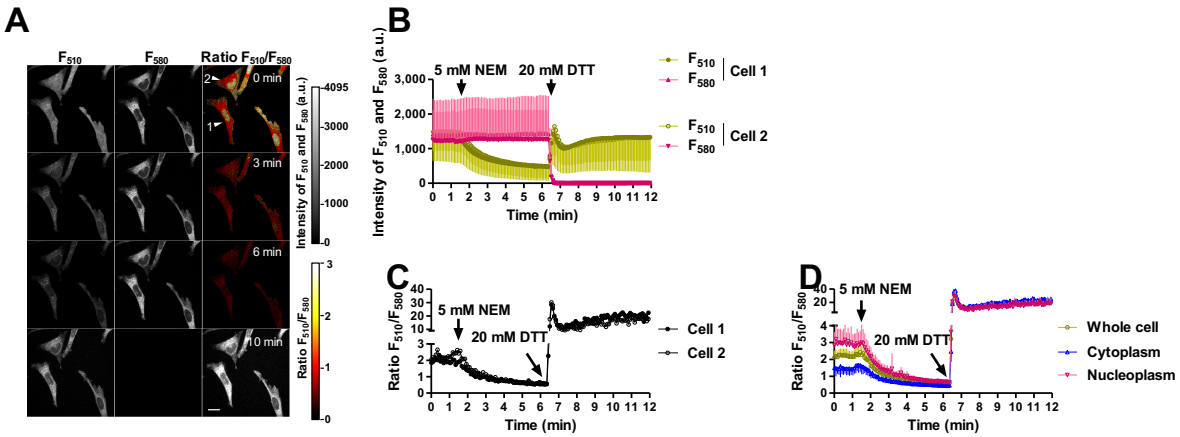

Figure S3. Reversible Reaction of FreSHtracer with Intracellular Thiols in Living Cells, Related to Figure 2

HeLa cells were equilibrated for 2 h with 5 μM FreSHtracer, and fluorescence emission intensities were monitored at F_{510} and F_{580} at 5-s intervals after treatment with *N*-ethylmaleimide (NEM), followed by 0.5 mM dithiothreitol (DTT). The F_{510}/F_{580} ratio (FR) was calculated using the NIS-Elements AR software program.

(A) Confocal and pseudo-color images of FreSHtracer-loaded cells.

(B and C) The fluorescence emission intensities of two cells (arrowheads) were monitored (B) and calculated as the FR (C).

(D) The average FR in whole cells, the cytoplasm, and the nucleoplasm from four different cells. All error bars represent the mean ± SEM.

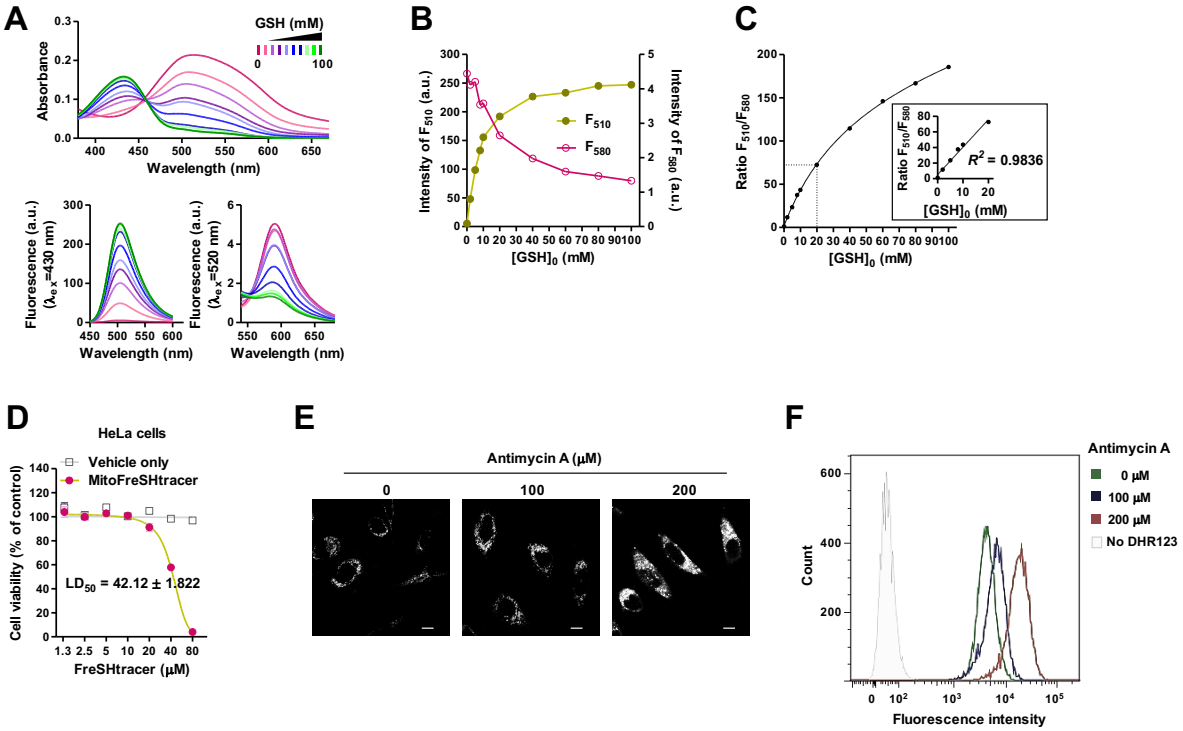

Figure S4. Characterization of MitoFreSHtracer, Related to Figure 2

(A–C) Spectroscopic properties of MitoFreSHtracer during the reaction with glutathione (GSH). Reactions were performed at room temperature in 10 mM phosphate buffer (pH 7.4) containing 150 mM NaCl and 2% dimethyl sulfoxide and monitored by ultraviolet-visible absorption spectroscopy. MitoFreSHtracer (10 μM) was reacted for 20 min with various concentrations of GSH ($[GSH]_0$ = 0–100 mM) (A). Fluorescence emission spectra of MitoFreSHtracer excited at 430 nm and 520 nm. Fluorescence intensities were plotted against the GSH concentration (B). The F_{510}/F_{580} ratio (FR) was calculated and plotted against the GSH concentration (C). A linear regression curve was fitted spanning the physiological range of GSH concentrations (0–20 mM; C, inset). a.u., arbitrary units.

(D) Effects of MitoFreSHtracer on cell viability. HeLa cells (5×10^3 cells/well; n = 3 independent biological replicates) were cultured for 18 h in 96-well dishes, and then treated for 24 h with either vehicle (dimethyl sulfoxide [DMSO]) or the indicated concentrations of FreSHtracer. Cell viability was analyzed using the MTT method. The LD_{50} values for FreSHtracer were calculated using GraphPad Prism 5. The error bars indicate the mean ± SEM.

(E and F) Measurement of the mitochondrial ROS generated by treatment with antimycin A. HeLa cells (1.8×10^4 cells/cm^2) were cultured for 18 h, and then incubated for 20 min with the indicated concentrations of antimycin A and 30 μM of dihydrorhodamine 123 (DHR123). Cells were washed twice with cold PBS, and analyzed in the presence of cold culture media by confocal microscopy (E) or with an LSR Fortessa flow cytometry system following trypsinization (F). Scale bar, 10 μm.

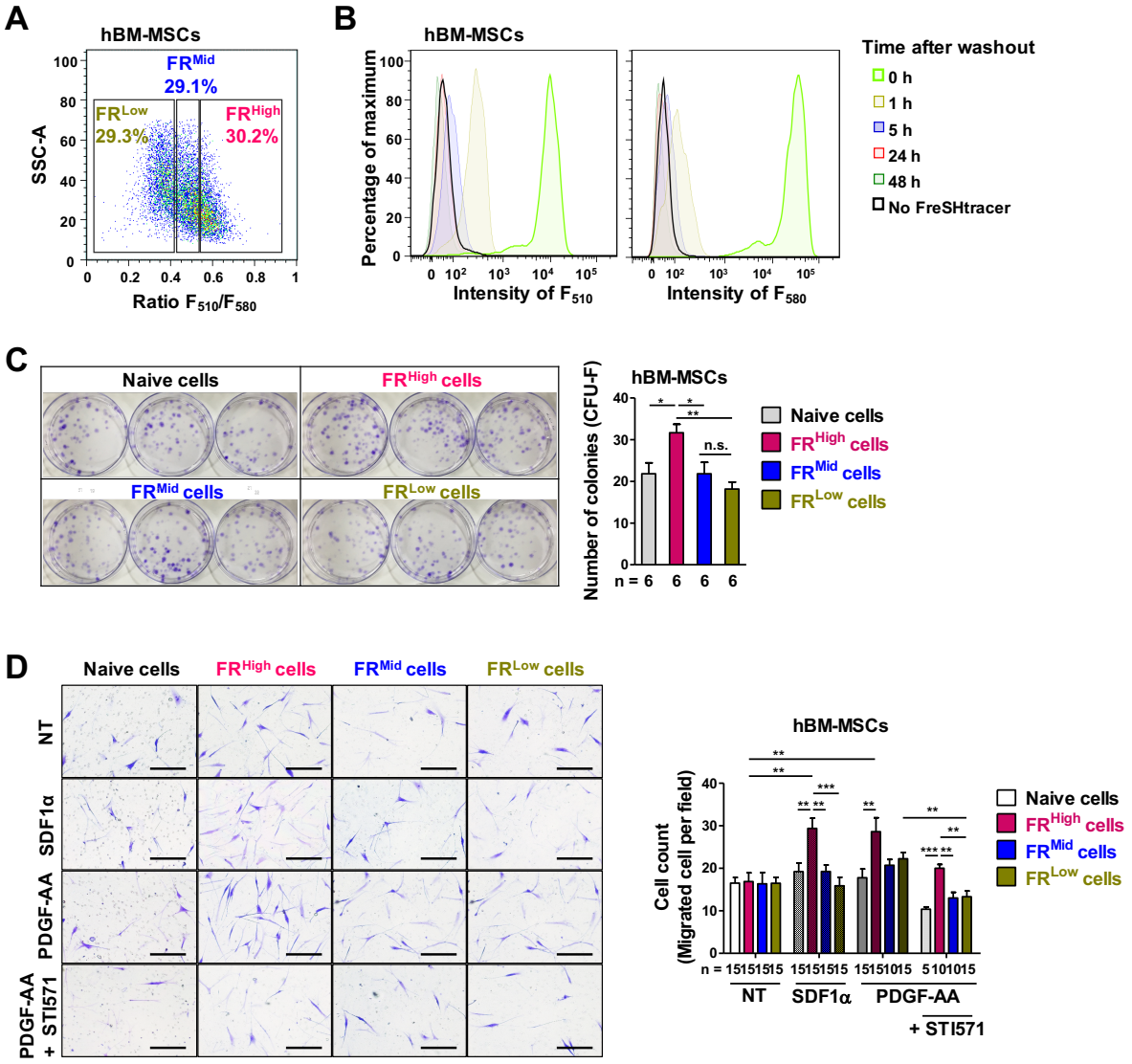

Figure S5. Characterization of Sorted hBM-MSCs According to F_{510}/F_{580} Ratio (FR) Values, Related to Figure 5

(A) Sorting of hBM-MSCs by FR into three populations: FR^{High}, FR^{Mid}, and FR^{Low} cells. Cells were characterized as described below, following the removal of FreSHtracer.

(B) Removal of FreSHtracer by PBS wash. hBM-MSCs were equilibrated with FreSHtracer (2 μM; 2 h), washed three times with PBS, and then cultured in growth media for the indicated times. Residual FreSHtracer in hBM-MSCs was measured by flow cytometry for F_{510} and F_{580}.

(C and D) Assays of colony-forming units-fibroblasts (CFU-F, n = 6 independent biological replicates; C) and chemotaxis (n = 5, 10, or 15 independent biological replicates; D) to stromal-derived factor 1-alpha (SDF1α, 150 ng/mL) and platelet-derived growth factor (PDGF)-AA (10 ng/mL) in the absence or presence of STI571 (0.5 μg/mL), a PDGFR inhibitor, for sorted hBM-MSCs according to FR and unsorted control (naive) cells. Scale bar, 200 μm. All error bars represent the mean ± SEM. $*P < 0.05$, $**P < 0.01$, $***P < 0.001$. n.s., not significant.

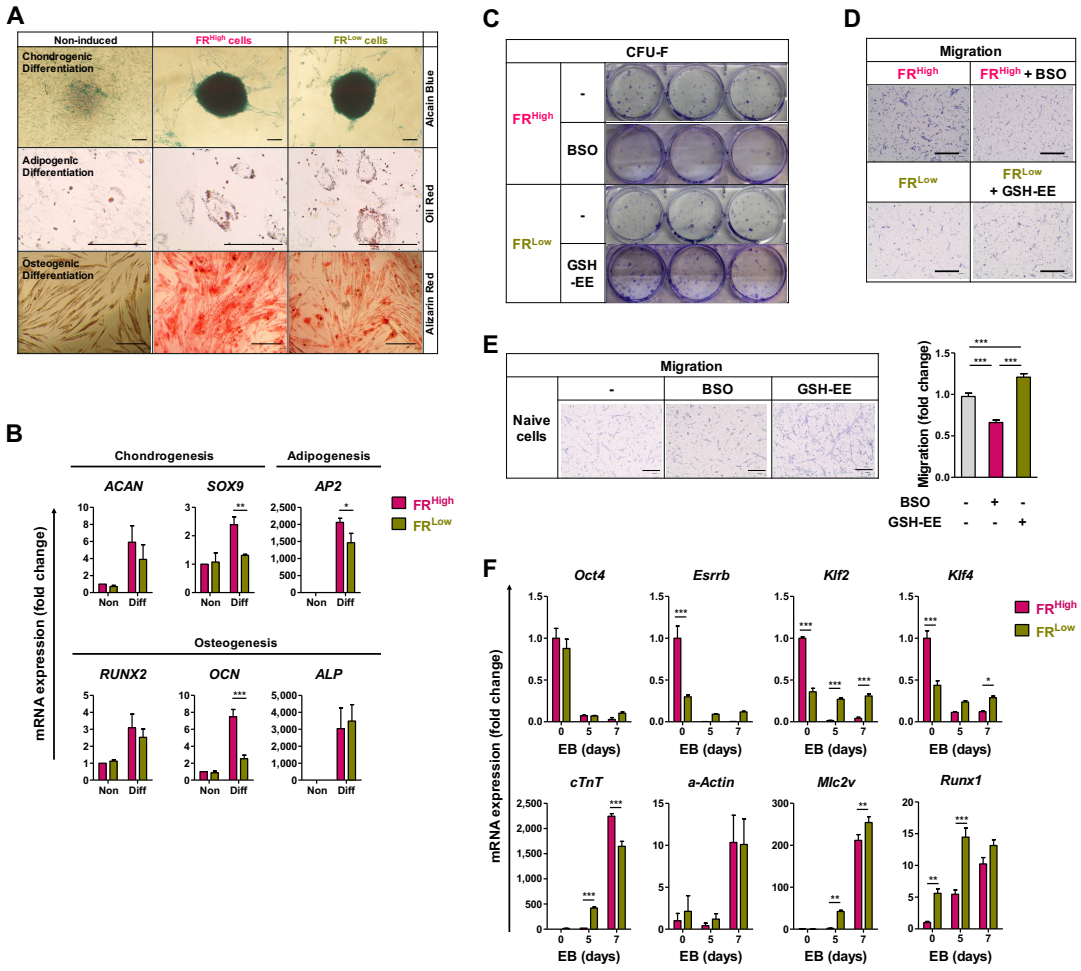

Figure S6. Cellular Functions of Sorted SCs According to F_{510}/F_{580} Ratio (FR) Values, Related to Figures 5 and 6

(A and B) Sorting of hES-MSC by FR into two populations: FR^{High} and FR^{Low} cells. Cells were cultured in chondrogenic, adipogenic, or osteogenic induction media. Cells were stained with Alcian Blue, Oil Red O, or Alizarin Red S (A). qPCR analysis (n = 4 independent biological replicates) to quantify lineage-specific genes in non-differentiated (Non) and differentiated (Diff) FR^{High} and FR^{Low} cells (B).

(C and D) Representative images for colony-forming unit fibroblasts assay (CFU-F, C) and chemotaxis assay to 10 ng/mL platelet-derived growth factor (PDGF)-AA (D) in FR^{High} and FR^{Low} hES-MSCs treated with BSO and GSH-EE, respectively. The corresponding graphs are shown in Figure 5J and 5K, respectively.

(E) Analyses of chemotaxis to 10 ng/mL PDGF-AA (n = 10 independent biological replicates) in unsorted control (naive) hES-MSCs treated with BSO or GSH-EE. Quantitative data are represented as the ratio to non-treated naive cells.

(F) mESC sorted by FR into two populations (FR^{High} and FR^{Low} cells) were differentiated by forming embryoid body (EB). qPCR analyses (n = 4 independent biological replicates) of the pluripotency and lineage-specific genes in cells from EB were performed at the indicated day. Quantitative data are represented as the ratio to FR^{High} cells of day 0. All error bars represent the mean ± SEM. $*P < 0.05$, $**P < 0.01$, $***P < 0.001$, one- or two-way ANOVA with Bonferroni post-hoc tests. Scale bar, 200 μm.

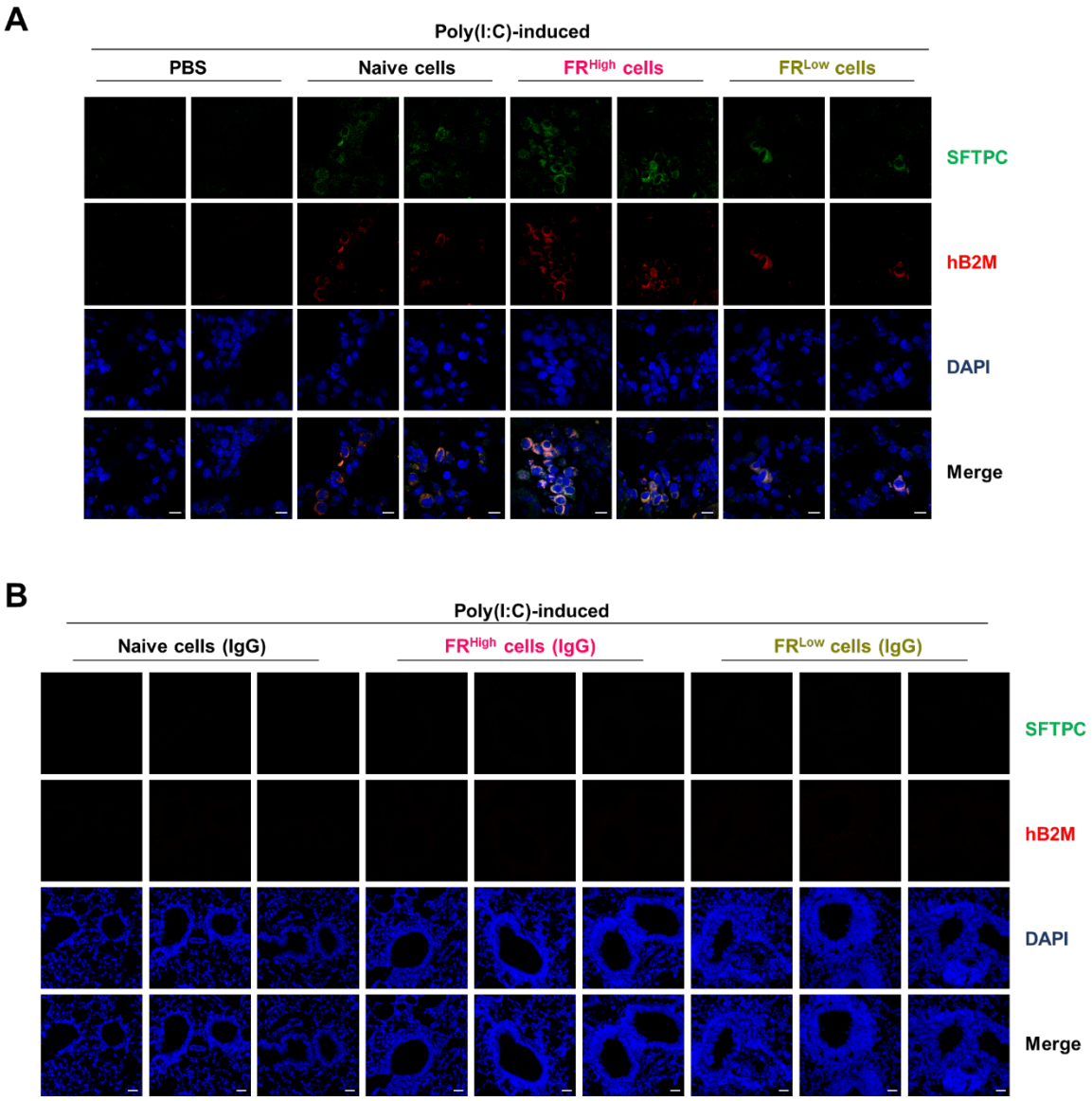

Figure S7. Immunostaining Analysis for Cellular Properties of Transplanted hES-MSCs, Related to Figure 7.

(A) Representative confocal images of lung tissue sections of poly(I:C)-induced asthma mice administrated with unsorted control (naive), FR^{High}, and FR^{Low} hES-MSCs or phosphate-buffered saline (PBS) after double staining for human β-2 microglobulin expressing cells (hB2M, red) and prosurfactant protein C (SFTPC, green) expressing type-2 alveolar cells. Nuclei were stained with DAPI (blue). (B) For negative control experiments, lung tissues of poly(I:C)-induced asthma animals administrated with the indicated hES-MSCs were co-stained with mouse and rabbit IgG control antibodies. Scale bar, 10 μm.

Table S1. K_D Values for Thiol Compounds Reacting with FreSHtracer
The K_D values of various thiols were determined as described in **Supplemental Experimental Procedures**.

Thiol compound	Structure	K_D (mM)
Glutathione	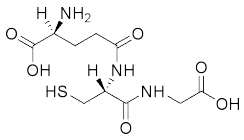	3.6 ± 0.3
Cysteine	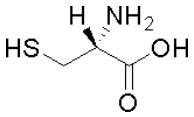	10.0 ± 0.7
Cysteamine	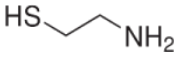	2.2 ± 0.4
β-mercaptoethanol	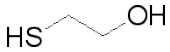	6.5 ± 0.5
Dithiothreitol	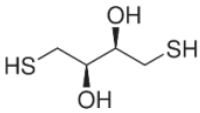	1.9 ± 0.2
N-acetyl cysteine	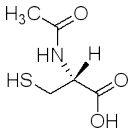	2.0 ± 0.4

Supplemental Experimental Procedures

Chemical synthesis of fluorescence probes

All of the chemicals used for probe synthesis were purchased from Sigma-Aldrich (St. Louis, MO) or TCI (Tokyo, Japan) and used without further purification. Dichloromethane was freshly dried via a solvent purification system (Glass Contour). Other solvents used were of anhydrous grade, obtained from Sigma-Aldrich or Acros (Geel, Belgium). Reactions requiring anhydrous conditions were performed under dry N_2. Silica gel (60 Å) was used for all column chromatography steps. Nuclear magnetic resonance (NMR) spectra were recorded at room temperature on Varian VNMRS400 or Mercury300 spectrometers. Chemical shifts are reported relative to the internal tetramethylsilane or residual solvent. Mass spectra were acquired at the National Center for Inter-University Research Facilities, Seoul National University. FreSHtracer was prepared according to our previously reported method (Cho and Choi, 2012). This probe is now commercially available (Cell2in, Seoul, Korea; http://www.cell2in.com).

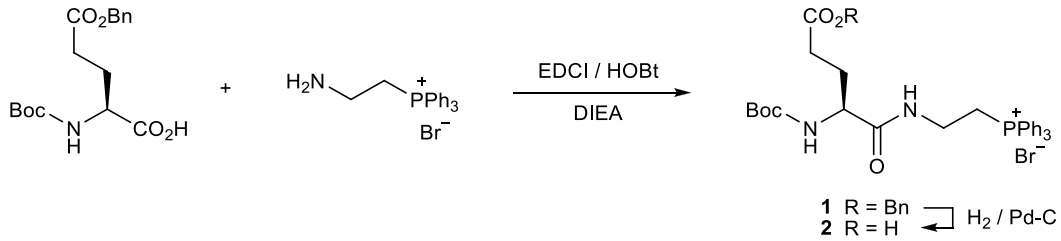

5-Benzyl *N*-(*tert*-butoxycarbonyl)-L-glutamate (0.10 g, 0.29 mmol), 1-hydroxybenzotriazole (HOBt, 80 mg, 2.0 eq.), and *N,N*-diisopropylethylamine (DIEA, 0.18 mL, 3.5 eq.) were dissolved in *N,N*-dimethylformamide (DMF, 1 mL). *N*-(3-dimethylaminopropyl)-*N'*-ethylcarbodiimide hydrochloride (EDCI, 0.11 g, 2.0 eq.) and (2-aminoethyl)-triphenylphosphonium bromide (Mari et al., 2013) (0.13 g, 1.2 eq.) were then added to the solution. After stirring for 16 h, the solution was diluted with ethyl acetate and then washed with 0.5 M citric acid, saturated $NaHCO_3$ aqueous solutions, and brine. The organic layer was dried over anhydrous Na_2SO_4 and concentrated under reduced pressure. The residue was purified by SiO_2 chromatography to obtain compound **1** as a white solid (0.16 g, 76%). ^{1}H NMR (400 MHz, $CDCl_3$): δ 9.49 (br s, 1H), 7.68–7.83 (m, 15H), 7.27–7.35 (m, 5H), 5.87 (d, J = 9.2 Hz, 1H), 5.08 (s, 2H), 4.18–4.23 (m, 1H), 3.61–3.87 (m, 4H), 2.43–2.47 (m, 2H), 2.12–2.22 (m, 1H), 1.94–2.01 (m, 1H), 1.43 (s, 9H); ^{13}C NMR (100 MHz, $CDCl_3$): δ 172.8, 172.7, 155.2, 135.8, 135.3 (d, $^4J_{CP}$ = 3.0 Hz), 133.4 (d, $^3J_{CP}$ = 10.4 Hz), 130.5 (d, $^2J_{CP}$ = 12.7 Hz), 128.4, 128.1, 128.0, 117.4 (d, $^1J_{CP}$ = 85.9 Hz), 79.2, 66.1, 53.9, 33.3, 30.4, 28.4, 28.3, 22.2 (d, $^1J_{CP}$ = 49.7 Hz); ^{31}P NMR (121 MHz, $CDCl_3$): δ 22.1; HRMS (*m/z*): $[M]^+$ calcd. for $C_{37}H_{42}N_2O_5P$, 625.2831; found. 625.2826.

Compound **1** (1.2 g, 1.7 mmol) was dissolved in the mixture of methanol (5 mL) and water (5 mL), and then 10 wt% Pd-C (0.12 g) was added to the solution. After stirring for 13 h under H_2 (1 atm), the reaction mixture was filtered through a Celite pad and the filtrate was concentrated under reduced pressure to give compound **2** as a white solid (1.04 g, 99%), which was used for the next reaction without further purification. ^{1}H NMR (400 MHz, $CDCl_3$): δ 8.95 (br s, 1H), 7.70–7.82 (m, 15H), 5.97 (br s, 1H), 4.16 (br s, 1H), 3.60–3.90 (m, 4H), 2.35–2.45 (m, 2H), 1.95–2.05 (m, 2H), 1.37 (s, 9H); ^{31}P NMR (121 MHz, $CDCl_3$): δ 22.1.

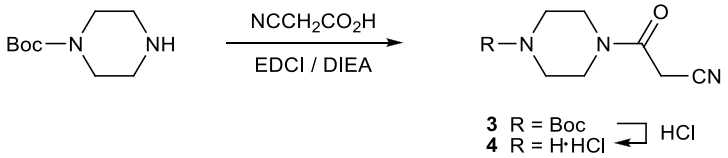

tert-Butyl pipeazine-1-carboxylate (1.0 g, 5.3 mmol) and cyanoacetic acid (0.54 g, 1.2 eq.) were dissolved in DMF (10 mL), and then DIEA (3.28 mL, 3.5 eq.) and EDCI (1.56 g, 1.5 eq.) were added to the solution. After stirring for 12 h, the solvent was evaporated under reduced pressure and the residue was purified by SiO_2 chromatography to give compound **3** as a white solid (1.13 g, 84%). ^{1}H NMR (400 MHz, $CDCl_3$): δ 3.60–3.64 (m, 2H), 3.50–3.55 (m, 2H), 3.51 (s, 2H), 3.43–3.48 (m, 4H), 1.47 (s, 9H); HRMS (*m/z*): $[M+H]^+$ calcd. for $C_{12}H_{20}N_3O_3$, 254.1505;

found. 254.1496.

Compound **3** (0.30 g, 1.2 mmol) was dissolved in a 4 M HCl dioxane solution (5 mL). After stirring for 1 h, the mixture was concentrated under reduced pressure to give compound **4** as a white solid in quantitative yield. This solid was used for the next reaction without further purification. ^{1}H NMR [400 MHz, dimethyl sulfoxide (DMSO)-d_6]: δ 9.54 (br s, 2H), 4.12 (s, 2H), 3.67–3.70 (m, 2H), 3.58–3.61 (m, 2H), 3.04–3.12 (m, 4H).

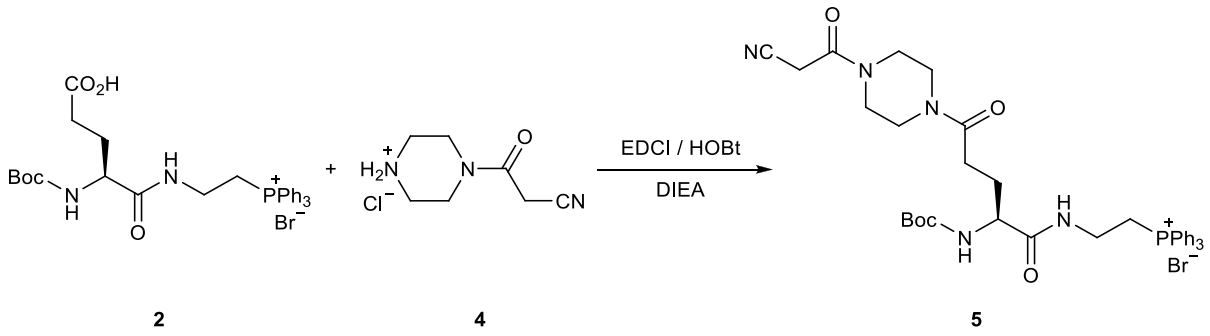

2 **4** **5**

Compound **2** (0.15 g, 0.24 mmol), compound **4** (49 mg, 1.05 eq.), and DIEA (0.15 mL, 3.5 eq.) were dissolved in DMF (2 mL), and then HOBt (3 mg, 0.1 eq.) and EDCI (95 mg, 2.0 eq.) were added to the solution. After stirring for 4 h, the solvent was evaporated under reduced pressure and the residue was purified by SiO_2 chromatography to give compound **5** as a yellowish-white solid (0.14 g, 78%). ^{1}H NMR (400 MHz, $CDCl_3$): δ (major conformer) 9.46 (br s 1H), 7.72–7.84 (m, 15H), 5.79 (d, J = 7.8 Hz, 1H), 4.15–4.21 (m, 1H), 3.47–3.79 (m, 14H), 2.50–2.60 (m, 2H), 2.12–2.15 (m, 1H), 2.00–2.04 (m, 1H), 1.42 (s, 9H); ^{13}C NMR (100 MHz, $CDCl_3$): δ (* major conformer; ** minor conformer) 172.8**, 172.7*, 171.2**, 171.0*, 161.1, 155.2, 135.3, 133.4 (d, $^3J_{CP}$ = 10.3 Hz), 130.5 (d, $^2J_{CP}$ = 12.7 Hz), 117.4 (d, $^1J_{CP}$ = 85.8 Hz), 114.5, 79.2, 54.0. 46.3*, 45.8**, 45.3*, 44.7**, 42.2**, 41.9*, 41.2**, 40.8*, 33.3, 30.0**, 29.5*, 29.2*, 28.9**, 28.3, 25.4, 22.2 (d, $^1J_{CP}$ = 49.8 Hz); ^{31}P NMR (121 MHz, $CDCl_3$): δ 22.1; HRMS (m/z): $[M]^+$ calcd. for $C_{37}H_{45}N_5O_5P$, 670.3158; found. 670.3157.

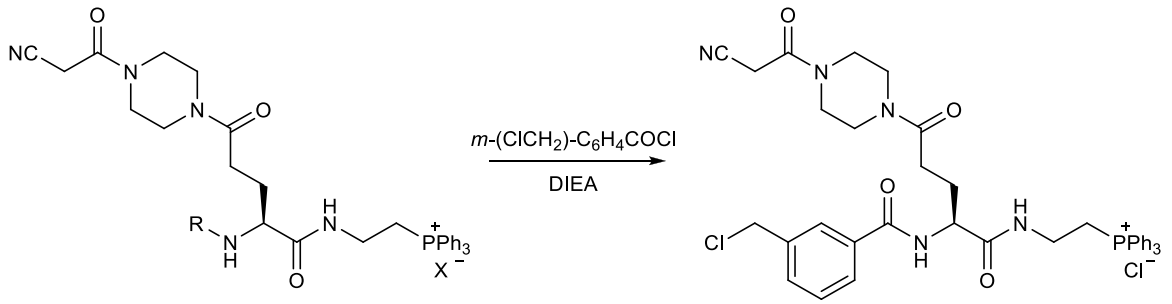

7

Compound **5** (0.23 g, 0.31 mmol) was dissolved in a 4 M HCl dioxane solution (3 mL). After stirring for 1 h, the mixture was concentrated under reduced pressure to give compound **6** as a yellowish-white solid in quantitative yield. This solid was used for the next reaction without further purification. ^{1}H NMR (400 MHz, DMSO-d_6): δ 9.44 (d, J = 6.1 Hz, 1H), 8.49 (br s, 3H), 7.76–7.94 (m, 15H), 4.09–4.11 (m, 1H), 3.80–3.84 (m, 2H), 3.33–3.50 (m, 12H), 2.50–2.55 (m, 2H), 1.94–1.98 (m, 2H); ^{31}P NMR (121 MHz, DMSO-d_6): δ 22.4.

Compound **6** (0.10 g, 0.15 mmol) and 3-(chloromethyl)benzoyl chloride (25 μL, 1.05 eq.) were dissolved in dichloromethane (1 mL), and DIEA (58 μL, 2.0 eq.) was added to the mixture. After stirring for 1 h, the solvent was evaporated under reduced pressure and the residue was purified by SiO_2 chromatography to give compound **7** as a white solid (0.10 g, 85%). ^{1}H NMR (400 MHz, $CDCl_3$): δ (major conformer) 9.65 (br s, 1H), 8.33 (d, J = 8.3 Hz, 1H), 8.13 (s, 1H), 8.05 (d, J = 7.8 Hz, 1H), 7.69–7.82 (m, 15H), 7.52 (d, J = 7.9 Hz, 1H), 7.42–7.46 (m, 1H), 4.74–4.79 (m, 1H), 4.65 (s, 2H), 3.35–3.74 (m, 14H), 2.53–2.60 (m, 2H), 2.25–2.30 (m, 2H); ^{13}C NMR (100

MHz, $CDCl_3$): δ ([*] major conformer; [**] minor conformer) 173.1[**], 173.0[*], 171.3[*], 171.2[**], 166.4, 160.9, 137.7, 135.5, 134.1, 133.5 (d, $^3J_{CP}$ = 10.3 Hz), 131.7, 130.6 (d, $^2J_{CP}$ = 12.7 Hz), 128.9, 128.3[*], 128.2[**], 127.8[*], 127.7[**], 117.5 (d, $^1J_{CP}$ = 85.9 Hz), 114.5, 54.2, 46.3[*], 45.9, 45.8[**], 45.3[*], 44.8[**], 42.1[**], 42.0[*], 41.3[**], 41.0[*], 30.2[**], 29.7[*], 28.3[*], 28.0[**], 25.3, 22.3 (d, $^1J_{CP}$ = 49.8 Hz); ^{31}P NMR (121 MHz, $CDCl_3$): δ 22.2; HRMS (*m/z*): $[M]^+$ calcd. for $C_{40}H_{42}ClN_5O_4P$, 722.2663; found. 722.2662.

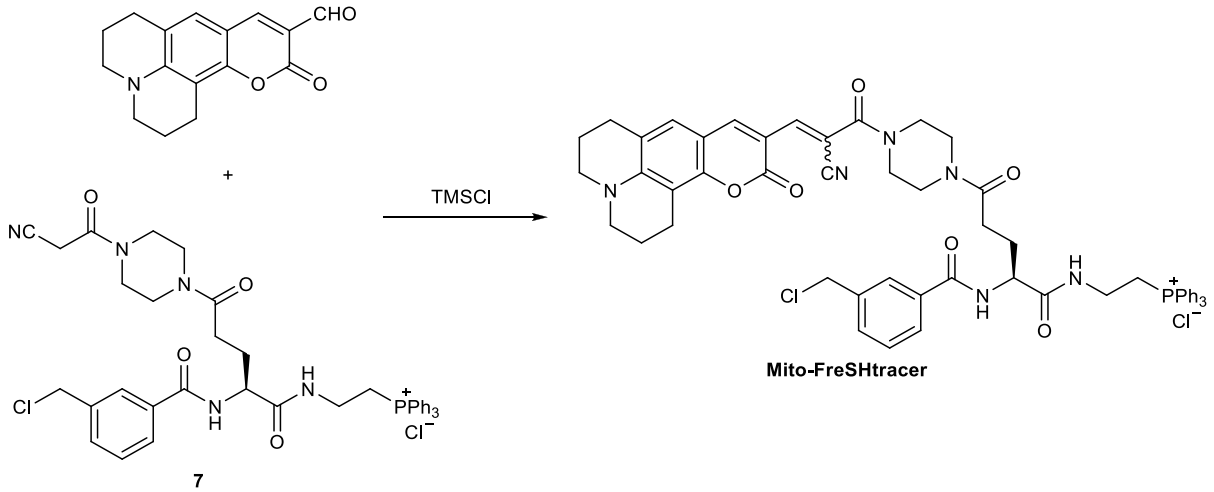

Compound **7** (0.12 g, 0.16 mmol) and 10-oxo-2,3,5,6-tetrahydro-1*H*,4*H*,10*H*-11-oxa-3a-azabenzo[*de*]anthracene-9-carbaldehyde (Yuan, 2011) (46 mg, 1.1 eq.) were dissolved in DMF (1 mL), and then chlorotrimethylsilane (60 μL, 3.0 eq.) was added to the solution (Ryabukhin S. V. , 2007). After stirring for 5 h at 130°C, the reaction mixture was concentrated under reduced pressure and the residue was purified by SiO_2 chromatography to give the final product as a red solid (79 mg, 50%). ^{1}H NMR (400 MHz, $CDCl_3$): δ (major isomer) 9.58 (br s, 1H), 8.63 (s, 1H), 8.40 (d, *J* = 7.4 Hz, 1H), 7.72–8.21 (m, 18H), 7.51 (d, *J* = 7.0 Hz, 1H), 7.42–7.45 (m, 1H), 7.00 (s, 1H), 4.74–4.80 (m, 1H), 4.60 (s, 2H), 3.58–3.73 (m, 12H), 3.33–3.38 (m, 4H), 2.83–2.87 (m, 2H), 2.72–2.78 (m, 2H), 2.55–2.58 (m, 2H), 2.27–2.31 (m, 2H), 1.97–2.04 (m, 4H); ^{13}C NMR (100 MHz, $CDCl_3$): δ (major isomer) 172.9, 171.1, 166.2, 163.9, 161.3, 152.5, 149.0, 145.9, 142.8, 137.6, 135.4, 134.0, 133.4 (d, $^3J_{CP}$ = 10.3 Hz), 131.6, 130.6 (d, $^2J_{CP}$ = 12.7 Hz), 128.8, 128.2, 127.7, 127.5, 119.9, 117.4 (d, $^1J_{CP}$ = 85.9 Hz), 117.1, 109.7, 108.2, 106.0, 100.4, 54.2, 50.4, 49.9, 45.9, 45.1 (br), 41.2 (br), 33.4, 29.9, 28.0, 27.2, 22.2 (d, $^1J_{CP}$ = 50.0 Hz), 20.9, 19.9, 19.8; ^{31}P NMR (121 MHz, $CDCl_3$): δ 22.2; HRMS (*m/z*): $[M]^+$ calcd. for $C_{56}H_{55}ClN_6O_6P$, 973.3609; found. 973.3616.

In vitro reactions of FreSHtracer with thiol compounds and reagents

Reactions between FreSHtracer and thiols were analyzed at room temperature with 10 μM FreSHtracer in a 10 mM phosphate buffer solution (PBS, pH 7.4) containing 150 mM NaCl and 2% (v/v) DMSO. The reaction was monitored by UV/Vis (Agilent 8453) and fluorescence (Hitachi F7000, or, Tecan Infinite 200Pro) spectroscopy. Fluorescence emissions were detected at 510 nm and 580 nm, exciting at 430 nm and 520 nm, respectively, to obtain the fluorescence ratio (FR; F_{510}/F_{580}). H_2O_2, glutathione (GSH), cysteine, cysteamine, N-acetylcysteine, ß-mercaptoethanol, dithiothreitol (DTT), diamide, buthionine sulfoximine (BSO), 3-(4,5-dimethylthiazolyl-2)-2,5-diphenyltetrazolium bromide (MTT), phorbol 12-myristate 13-acetate (PMA), NADPH, 1-chloro-2,4-dinitrobenzene (CDNB), and Ellman's reagent were purchased from Sigma-Aldrich. Yeast glutathione reductase was purchased from Calbiochem.

Calculation of the K_D values for thiol compounds

Mixtures of FreSHtracer (10 μM) with various concentrations of thiols were prepared in 10 mM PBS containing 150 mM NaCl and 2% (v/v) DMSO. To adjust the pH, acetate (4.0 and 5.0), CHES (9.0 and 10.0), or phosphate (other pH values) buffers were used. Fluorescence emission spectra were recorded 20 min after preparation of the mixtures. The emission intensities at 510 nm, over a range of thiol concentrations, were curve-fitted to an equation [1] describing the theoretical relation between the fluorescence intensity at equilibrium (F_{eq}) and the dissociation constant (K_D):

$$F_{eq} = k\{[\text{FreSH}]_T + [\text{thiol}]_T + K_D - \sqrt{([\text{FreSH}]_T + [\text{thiol}]_T + K_D)^2 - 4[\text{FreSH}]_T[\text{thiol}]_T}\} \quad [1]$$

In equation [1], $[\text{FreSH}]_T$ and $[\text{thiol}]_T$ denote the total concentrations of FreSHtracer and thiol, respectively.

Calculation of the rate constants for the reactions between FreSHtracer and thiols

FreSHtracer was added to GSH or protein solution in reaction buffer, and fluorescence emission (F_{510}) was detected at 510 nm with excitation at 430 nm. The kinetic experiments were performed using an initial FreSHtracer concentration of 10 μM. The data were analyzed using SigmaPlot 2000 (SPSS) and fitted to equation [2], which describes how the fluorescence intensities change as the reaction approaches equilibrium:

$$F(t) = F_0 + F_{eq}(1 - e^{(k_f[\text{thiol}]_T + k_r)t}) \quad [2]$$

In equation [2], F_0 and F_{eq} are the fluorescence intensities at the beginning of the reaction and at equilibrium, respectively; k_f and k_r are the rate constants for the forward and reverse reactions, respectively; and $[\text{thiol}]_T$ is the total concentration of either GSH or PSH. The reactive thiol concentrations of PSH solutions were measured by performing Ellman's assay. The reactions were performed at room temperature in 10 mM PBS (pH 7.4) containing 150 mM NaCl and 2% DMSO.

Preparation of protein solutions

HeLa cells were cultured for two days in a 150-mm dish. After reaching 80% confluence, the cells were harvested by scraping in PBS, followed by centrifugation. To prepare a protein solution, the cells were resuspended in PBS containing 0.1% Triton X-100 and completely disrupted by sonication. Following centrifugation at 12,000 × *g* for 10 min at 4°C, the lysates were dialyzed in cold PBS to remove low-molecular-weight thiol species, including GSH. The protein concentration was determined by the bicinchoninic acid method. These preparations were used as protein (PSH) solutions in further experiments.

In vitro measurement of GSH levels

To determine the GSH concentrations in BSO-treated HeLa cells, the cells were cultured in 96-well plates (White clear bottom, Corning) and then treated with BSO for 48 h. After washing twice with Hanks' buffered salt solution, the total GSH and GSSG concentrations were determined using a GSH/GSSG-Glo Assay kit (Promega). The concentration of reduced GSH was determined by subtracting the GSSG concentration from the total GSH concentration. Calculation of intracellular GSH concentrations in HeLa cells was based on an estimated average cell volume of 2600 μm^3 (Zhao et al., 2008) and total cell numbers.

MTT colorimetric assays

HeLa cells (5×10^3 cells/well), hBM-MSCs (1.3×10^3 cells/well), and hES-MSCs (1×10^4 cells/well) were cultured in 96-well dishes for 18 h and treated for 24 h with either DMSO or various concentrations of FreSHtracer. After washing with PBS, the cells were incubated for 3–4 h in MTT solution (500 μg/mL in culture medium). The MTT solution was removed, and DMSO was added to dissolve the formazan crystals. The 96-well dishes were incubated in the dark, and then the absorbance at 570 nm in each well was measured on a microplate spectrophotometer. Each treatment was performed in triplicate.

Stem cell culture and characterization in vitro and in vivo

hES-MSCs were grown in EGM2-MV medium (Lonza, Walkersville, MD) in tissue culture dishes coated with a type-I collagen from the rat tail (Sigma-Aldrich, St. Louis, MO; 150 μg per 100-pi dish), as previously described (Hong et al., 2015). hBM-MSCs (Lonza, Walkersville, MD) were cultured according to the manufacturer's instructions. The cells were loaded with 2 μM FreSHtracer for 2 h in culture medium and were subsequently sorted at 4°C according to their FR levels using an AriaIII Flow Cytometer System (BD Biosciences, San Jose, CA). FR^{High}, FR^{Mid}, and FR^{Low} fractions were collected and prepared for further analyses. The fluorescence intensities of cells were detected at Ex405-Em525/50 and Ex561-Em582/15. The sorted cells were washed twice with 50 mL PBS to remove the FreSHtracer from the cells and then further cultivated in culture medium for 24 h prior to conducting functional in vitro or in vivo experiments, as described below. Monitoring of intracellular FR changes following H_2O_2 treatment was achieved by confocal microscopy, as described in the main text. In vitro assays for cell proliferation, colony-forming unit-fibroblast (CFU-F), multipotency (in vitro differentiation into chondrogenic, adipogenic, or osteogenic lineages), and cell migration were performed as previously described (Kang et al., 2015). Chemotactic activity was measured using Boyden chambers with 8-μm pores (Corning, Corning, NY) in which 10 ng/mL platelet-derived growth factor (PDGF)-AA; R&D Systems, Minneapolis, MN) or 150 ng/mL stromal-derived factor 1-alpha (SDF1α; R&D Systems, Minneapolis, MN) was added to the lower chamber. To inhibit the PDGF signaling cascade, we used STI571 (Selleckchem, Houston, TX), a PDFGFR inhibitor. The stained cells on the lower side of the membranes were quantified by digital image analysis using Image Pro 5.0 software (Media-Cybernetics, Rockville, MD).

To evaluate the in vivo therapeutic potency of the sorted hES-MSCs, we generated a murine model of severe asthma as follows. Six-week-old BALB/c mice (OrientBio, Gapyong, Gyeonggi-do, Korea) were sensitized and challenged by intranasal administration with 75 μg ovalbumin (OVA; Sigma-Aldrich, St. Louis, MO) and 10 μg of polyI:C (Calbiochem, San Diego, CA) at days 0, 1, 2, 3, 7, 14, 21, 22, and 23. The mice were injected intravascularly with 3×10^5 hES-MSCs sorted according to the FR (as described above) on day 15. Histological examination and bronchoalveolar lavage fluid analysis were performed as previously described (Jin et al., 2016). The engraftment of the administrated hES-MSCs was determined by immunofluorescence analysis of human β2-microglobulin (primary mouse monoclonal antibody, Santa Cruz Biotechnology, Dallas, TX) and visualized using an Alexa546-labeled anti-mouse secondary antibody (Invitrogen, Carlsbad, CA). The differentiation lineage was evaluated by co-staining for human β2-microglobulin and prosurfactant protein C (rabbit polyclonal, Abcam, Cambridge, UK), as visualized with an Alexa488-labeled anti-mouse secondary antibody (Invitrogen, Carlsbad, CA). Nuclei were counterstained using 4′6-diamino-2-phenylinodole (DAPI; Sigma-Aldrich, St. Louis, MO). Stained samples were photographed on an inverted fluorescence microscope (EVOS FL Color Imaging System, Life Technologies) or Zeiss LSM780 AxioObserver.Z1 confocal microscope system (Carl Zeiss, Munich, Germany). All animal experiments were approved and performed in accordance with guidelines set by the Institutional Animal Care and Use Committee of the University of the Ulsan College of Medicine (2015-12-061).

Quantitative PCR

The primers for human and mouse transcripts were as follows.

Genes	Forward	Reverse
For human genes		
GAPDH	ACCCACTCCTCCACCTTTGA	TGTTGCTGTAGCCAAATTCGTT
OCT4	GAGCCCTGCACCGTCACC	TTGATGTCCTGGGACTCCTCC
SOX2	TACAGCATGTCCTACTCGCAGC	GAGGAAGAGGTAACCACAGGGG
CXCR4	ACTACACCGAGGAAATGGGCT	CCCACAATGCCAGTTAAGAAGA
cMET	AGCGTCAACAGAGGGACCT	GCAGTGAACCTCCGACTGTATG

PDGFRA	TTGAAGGCAGGCACATTTACA	GCGACAAGGTATAATGGCAGAAT
PDGFRB	TGATGCCGAGGAACTATTCATCT	TTTCTTCTCGTGCAGTGTCAC
VEGFR1	CTCTCTCCCTGATCGGTGACA	GGAGGGCAGAGCTGAGTGTTAG
VEGFR2	GGTTGCATTACTGTACCCATCATTT	TGAGATGGAATCTGACCATGTTG
ANGPT1	TGCTCACGTGGCTCGACTATA	AGCACAGCAAGCTCAGCAGTTT
CSF1	TGCTGGAGAAGGTCAAGAATGTC	GTTGTTGCAGTTCTTGCTGAAAA
IDO1	TCCGTGAGTTTGTCCTTTCAAA	CAGGGAGACCAGAGCTTTCACA
AP2	GGGTCACAGCACCCTCCTGA	GGTTTGGCCATGCCAGCCAC
ACAN	AGCCTGCGCTCCAATGACT	TAATGGAACACGATGCCTTTCA
SOX9	TTCCGCGACGTGGACAT	TCAAACTCGTTGACATCGAAGGT
RUNX2	TCTTAGAACAAATTCTGCCCTTT	TGCTTTGGTCTTGAAATCACA
OCN	AGCAAAGGTGCAGCCTTTGT	GCGCCTGGGTCTCTTCACT
ALP	GACCTCCTCGGAAGACACTC	TGAAGGGCTTCTTGTCTGTG
For mouse genes		
Gapdh	AGGTCGGTGTGAACGGATTTG	TGTAGACCATGTAGTTGAGGTCA
Oct4	GAAGCAGAAGAGGATCACCTTG	TTCTTAAGGCTGAGCTGCAAG
Sox2	GCTCGCAGACCTACATGAACG	GCCTCGGACTTGACCACAGA
Nanog	CTTTCACCTATTAAGGTGCTTGC	TGGCATCGGTTCATCATGGTAC
cMyc	TCTCCATCCTATGTTGCGGTC	TCCAAGTAACTCGGTCATCATCTC
Klf2	AGGCCTGTGGGTTCGCTATAA A	GGCAAATTATGGCTCAAAGTAGCAG
Klf4	CCATTATCAAGAGCTCATGCCA	GTTTTGCCACAGCCTGCATAG
Rex1	TCCATGGCATAGTTCCAACAG	TAACTGATTTTCTGCCGTATGC
Esrrb	TGGGCCTAGCAGGGTCAGA	TGCCACCTGTTTCTCATGAGTAG
Neurog2	TGTAAGGGTTGAATGCAAGCGTGG	GTGTGTGGCTGATCCTGGCAATGC
Olig2	GAGCACTGCACTTGACTTCTTTCC	AGGACCCTAAGTGCTTCTGATACC
T	GCTTCAAGGAGCTAACTAACGAG	CCAGCAAGAAAGAGTACATGG
Nkx2.5	CTTCAAGCAACAGCGGTACCT	CGCTGTCGCTTGCACTTGTA
Neurog1	GGTTTGGAAAAGGGACAGATGAGC	AAGCCTTGCCATTGTATTGTCAGC
Neurod1	AGGGGATCAAAGTTCCTGTTCACC	AGGTCACAGGTAGTAAAATGCTGG
Nkx2.2	GGAGCACAATCTGGTCATCTGTGG	CAGTTGACATCCACAAGGCAGACG
Ascl2	CCAAATGCCAAGTGCTGACTGACC	CAGAGGTCATCTTTATTGTGCTCC
Gfap	TGTACTAACAGAGCGAGCCTATGC	GGGACTTGCTGCCTTTAACATTGG
S100b	TGGACTTGAGGCTTTCTAACTTGC	ATGCGAAGGCATTGTTCAGTTGAC
Atoh	TGGGAGTTCATCCTTGCGTGTTGC	AGACACACTGCTGGACACACTTGG
Mlc2v	TCAGCTGCATTGACCAGAAC	CCCGAAGAGTGTGAGGAAGA
Runx1	GAGATTCAACGACCTCAGGTTT	TGTAAAGACGGTGATGGTCAGA
a-Actin	GTGTGACATCGATATCCGCAAA	GAAGCACTTGCGGTGGACAATG
cTnT	TGAAGAAGCCAAAGATGCTGAA	CACCAAGTTGGGCATGAAGAG
Tnfa	CCCTCACACTCAGATCATCTTCT	GCTACGACGTGGGCTACAG
Ccl2	GGCTCAGCCAGATGCAGTTAA	CCAGCCTACTCATTGGGATCA
Il1b	CTACAGGCTCCGAGATGAACAAC	GTCCATTGAGGTGGAGAGCTTTC
Il12a	GTGGCCATCGATGAGCTGAT	TCTGCTTCTCCCACAGGAGGTT
Il18	GACTCTTGCGTCAACTTCAAGG	CAGGCTGTCTTTTGTCAACGA

Reactions were performed with a KAPA SYBR FAST qPCR Kit (Kapa Biosystems) using a CFX96TM Real-Time system (Bio-Rad).

Western blotting

Cell lysates were prepared in lysis buffer (50 mM Tris, pH 7.5, 150 mM NaCl, 1 mM ethylenediaminetetraacetic acid, 1% Triton X-100, and a Roche protease inhibitor cocktail), resolved via sodium dodecyl sulfate-polyacrylamide gel electrophoresis, and transferred to a nitrocellulose membrane. The primary antibodies used were: Oct4 (SC5279, Santa Cruz Biotechnology, Dallas, TX), Nanog (RCAB001P, ReproCELL, Kanagawa, Japan), Sox2 (Ab92494, Abcam, Cambridge, UK), Klf4 (4038, Cell Signaling Technology, Danvers, MA), and β-

actin (A5441, Sigma-Aldrich, St. Louis, MO). The secondary antibody was goat anti-rabbit IgG-HRP (sc-2004) or goat anti-mouse IgG-HRP (sc-2005), both from Santa Cruz Biotechnology (Dallas, TX).

Supplemental References

Cho, A.Y., and Choi, K. (2012). A coumarin-based fluorescence sensor for the reversible detection of thiols. Chem Lett *41*, 1611-1612.

Filonov, G.S., Piatkevich, K.D., Ting, L.M., Zhang, J., Kim, K., and Verkhusha, V.V. (2011). Bright and stable near-infrared fluorescent protein for in vivo imaging. Nat Biotechnol *29*, 757-761.

Hong, K.S., Bae, D., Choi, Y., Kang, S.W., Moon, S.H., Lee, H.T., and Chung, H.M. (2015). A porous membrane-mediated isolation of mesenchymal stem cells from human embryonic stem cells. Tissue Eng Part C Methods *21*, 322-329.

Jin, H.J., Lee, H.J., Heo, J., Lim, J., Kim, M., Kim, M.K., Nam, H.Y., Hong, G.H., Cho, Y.S., Choi, S.J.*, et al.* (2016). Senescence-associated MCP-1 secretion is dependent on a decline in BMI1 in human mesenchymal stromal cells. Antioxid Redox Signal *24*, 471-485.

Kang, H., Kim, K.H., Lim, J., Kim, Y.S., Heo, J., Choi, J., Jeong, J., Kim, Y., Kim, S.W., Oh, Y.M.*, et al.* (2015). The therapeutic effects of human mesenchymal stem cells primed with sphingosine-1 phosphate on pulmonary artery hypertension. Stem Cells Dev *24*, 1658-1671.

Mari, M., Morales, A., Colell, A., Garcia-Ruiz, C., Kaplowitz, N., and Fernandez-Checa, J.C. (2013). Mitochondrial glutathione: features, regulation and role in disease. Biochim Biophys Acta *1830*, 3317-3328.

Ryabukhin S. V. , P.A.S., Volochnyuk D. M. , Pipko S. E., Shivanyuk A. N., and Tolmachev A. A. (2007). Combinatorial Knoevenagel reactions. J Comb Chem *9*, 1073–1078.

Yuan, L., Lin, W. Y., Song, J. Z. & Yang, Y. T. (2011). Development of an ICT-based ratiometric fluorescent hypochlorite probe suitable for living cell imaging. Chem Commun *47*, 12691–12693.

Zhao, L., Kroenke, C.D., Song, J., Piwnica-Worms, D., Ackerman, J.J., and Neil, J.J. (2008). Intracellular water-specific MR of microbead-adherent cells: the HeLa cell intracellular water exchange lifetime. NMR Biomed *21*, 159-164.